 doi:10.20944/preprints202207.0110.v1

Article

An Account of Models of Molecular Circuits for Associative Learning with Reinforcement Effect and Forced Dissociation

Zonglun Li[1,2*], Alya Fattah [1], Peter Timashev[3] and Alexey Zaikin [1,2,3,4]

[1] Department of Mathematics, University College London, London, United Kingdom
[2] Institute for Women's Health, University College London, London, United Kingdom
[3] World-Class Research Center "Digital Biodesign and Personalized Healthcare", Sechenov University, Moscow 119991, Russia
[4] Lobachevsky State University of Nizhny Novgorod, Nizhny Novgorod, Russia
* Correspondence: zonglun.li.20@ucl.ac.uk

Abstract: The development of synthetic biology has enabled us to make massive progress on biotechnology and to approach research questions from a brand new perspective. In particular, the design and study of gene regulatory networks *in vitro*, *in vivo* and *in silico*, have played an increasingly indispensable role in understanding and controlling biological phenomena. Among them, it is of great interest to understand how associative learning is formed at the molecular circuit level. Noticeably, mathematical models have been increasingly used to predict the behaviors of molecular circuits. The Fernando's model, which is thought to be one of the first works in this line of research using the Hill equation, attempted to design a synthetic circuit that mimics Hebbian learning in the neural network architecture. In this article, we carry out in-depth computational analysis of the model and demonstrate that the reinforcement effect can be achieved by choosing the proper parameter values. We also construct a novel circuit that can demonstrate forced dissociation, which was not observed in the Fernando's model. Our work can be readily used as reference for synthetic biologists who consider implementing the circuits of this kind in biological systems.

Keywords: associative learning; molecular circuits; synthetic biology; mathematical modeling; Hill equation; Pavlov's dog; reinforcement; dissociation; non-dimensionalization

1. Introduction

Synthetic biology is an emerging field that involves re-engineering the existing biological systems or creating new ones that may solve real-world problems in medicine, agriculture, etc [1–9]. Over the past few decades, synthetic biology has witnessed rapid revolution in biotechnology industry and opened up enormous potential for next-generation research in biology due to the increasingly tremendous power of genetic engineering technology and ever decreasing cost of synthesis and sequencing [10–17]. Particularly, increasing attention has been drawn to designing and testing synthetic biological circuits *in vitro*, *in vivo* and *in silico*, in an attempt to better understand bio-artificial intelligence at cellular and molecular level [18–23]. These artificial circuits can therefore function as fundamental units to modify existing cellular behaviors and to perform a wide range of tasks of our own interest in programmable organisms [24–28]. Notably, numerous synthetic circuits have been developed for the decision-making tasks such as classification and associative learning [29–34]. Besides, with the growing collaboration between theorists and experimentalists in almost every discipline, we also noticed a trend in synthetic biology that mathematical models have been frequently used to acquire insight, inform troubleshooting and make predictions [35–39].

It is believed that associative learning occurs in many aspects of our life and is regarded as the basis for our understanding of other forms of behavior and cognition in human and nonhuman animals [40–44]. The most classic experiment on associative learning is

 doi:10.20944/preprints202207.0110.v1

Pavlov's dog, in which the dog managed to associate the ring of a bell with the smell of the food [45,46]. The dog learned to associate the conditioned stimulus (bell's ring) with the unconditioned stimulus (smell) such that next time, in the presence of the bell's ring alone, the dog knows the food will be served soon and the learned response (saliva from its mouth) is observed. The historical viewpoint is that mammalian nervous system plays a vital role in associative learning through neuronal signaling and re-configuration [47–50].

However, some studies have revealed the possibility that non-neural agents may also organize in a similar fashion [34,51,52]. Naturally, one can reckon that molecular circuits may display similar behaviors as molecular reactions form the building block of cellular activities. As a result, the design and investigation of molecular interactions that manifest associative learning has become an active research topic. Although logic gates have been widely adopted in synthetic biology for emulating diverse biological behaviors [53–57], in this article, the focus is confined to the continuous models constructed by the Hill equation [58,59] since continuous models tend to generate more accurate results and facilitate the comprehension of fine details of the system. One of the first models is the Fernando's model where the authors designed a genetic circuit that mimics Hebbian learning in the neural network architecture [60]. The work stands as a well-organized interdisciplinary article in which a mathematical model is developed and the biotechnological approach that the model can be implemented in *Escherichia coli* is thoroughly discussed. Nonetheless, because of its interdisciplinary nature, the work only demonstrates the fact that learning can be formed after conditioning but fails to investigate other more advanced behaviors such as reinforcement effect and forced dissociation. More specifically, it is natural to assume that the learned response gets stronger with the increasing times of conditioning. For illustrative brevity, we name the phenomenon *reinforcement effect*. Besides, it is reasonable to suppose that the response gets weaker with the repeated cuing of conditioned stimulus (with no unconditioned stimulus taking place at the same time) shortly after the formation of conditioning and we call it *forced dissociation*. To the best of our knowledge, neither of them has been formally discussed in the previous literature. The potential importance of these two behaviors can be explained by two aspects. On the one hand, in Pavlov's dog's experiment, the former would be equivalent to the scenario that the repeated conditioning of the bell and the food would reinforce the dog's belief that the bell's ring is a reminder of food availability; and the latter would be that the repeated bell's ring alone shortly after the conditioning would stop the dog reckoning that the bell is related to the food's availability. On the other hand, these properties may provide experimentalists with more flexibility over the control of some biological systems as synthetic circuits are widely used to regulate them [4,6,61,62]. We will show that the Fernando's model is able to manifest reinforcement effect by choosing the proper parameters but unable to manifest forced dissociation. This motivated us to design a new circuit that possesses the potential to display forced dissociation. The new circuit also involves fewer proteins and doesn't contain any feedback loop, which can potentially reduce the wiring complexity in the practical implementation. In the meantime, we will also study the robustness of the respective models to the Hill coefficients as this will instruct experimentalists on the type of polymers that can be used to implement the circuit.

2. Models

2.1. Fernando's Model

The circuit diagram of the Fernando's model is shown in Figure 1 and we assume that the circuit can be implemented in a programmable cell. Unlike the schematic diagram given in [60], here we omit genes for the illustrative simplicity. In the diagram, each oval box denotes a particular protein. The activation is drawn with an arrow and the inhibition is drawn with a hammerhead. Except for the inhibition $u_1 \to r_1$ and $u_2 \to r_2$ where the input molecules are directly bound to the repressors, all the other activation and inhibition are realized by transcription and translation. For instance, repressor r_1 inhibits the transcription of a particular gene which guides the manufacturing of molecule ω_1. Also

Preprints (www.preprints.org) | NOT PEER-REVIEWED | Posted: 7 July 2022 doi:10.20944/preprints202207.0110.v1

note that the upstream gene of the protein p has two available operator sites, one for r_1, ω_1, and another for r_2, ω_2. More detailed explanation can be found in [60]. The Fernando's model is characterized by the system as follows ($N = 2$):

$$\begin{cases} \dfrac{dp}{dt} = \displaystyle\sum_{j=1}^{N} v_p \Big(\frac{\omega_j^a}{K_\omega^a + \omega_j^a}\Big)\Big(\frac{K_r^b}{K_r^b + r_j^b}\Big) - \delta_p p \\ \dfrac{d\omega_j}{dt} = v_\omega \Big(\dfrac{p^b}{K_p^b + p^b}\Big)\Big(\dfrac{K_r^b}{K_r^b + r_j^b}\Big) - \delta_\omega \omega_j + \epsilon_j \\ r_j = \dfrac{R}{1 + k u_j} \end{cases} \tag{1}$$

In the equations above, u_1 and u_2 represent the respective concentrations of the unconditioned stimulus and the conditioned stimulus and they will be given to the cell in a transient time window. ω_1 and ω_2 represent the respective concentrations of the weight molecules. r_1 and r_2 represent the respective concentrations of the repressor molecules. The concentration of the response molecule is denoted by p. K_ω, K_r and K_p denote the respective Hill constants for molecule ω, r and p that measure the concentration of transcription factors required for half occupancy. R denotes the repressor concentration in the absence of molecule u. a and b are Hill coefficients which measure the cooperativity of the transcriptional factor. In [60], the authors use $a = 4$ and $b = 2$ but in this work, we will study the impact of varying integer values of a and b on the qualitative behaviors. ϵ denotes the basal grow rate and we assume that it is only non-zero for $j = 1$. v and δ denote the growth and degradation rate parameter respectively and the subscripts are used to signify the source of contribution. As one can observe from the architecture, the genetic circuit is structurally symmetric and the left and the right half are independent. The association is triggered by the feedback of the response molecule p and the inspiration came from the Hebbian learning which has been thought to dictate the information exchange between neurons [63].

In order for the association to be formed, we can simply make the concentration of the molecule ω_1 abundant and the molecule ω_2 insignificant before the start of the experiment. When only molecule u_1 is given to the cell, it binds to the repressor molecule r_1 and reduces the concentration of the molecule r_1. Therefore, the inhibition on the transcription with respect to the genes controlled by molecule r_1 will be lifted. Eventually, sufficient molecule ω_1 will activate the transcription with respect to the gene associated with the response molecule p and promote the production of p. Conversely, when only molecule u_2 is given to the cell, we won't be able to observe abundant molecule p due to the shortage of ω_2 availability. However, the time when molecule u_1 is paired with molecule u_2, the production of molecule p (triggered by u_1) will elevate the concentration of molecule ω_2 because of the feedback loop so that the next time even when only molecule u_2 is present, there will already exist sufficient molecule ω_2 for the production of p which implies that the association has been formed.

In order to analyze a system of differential equations, one often converts the system to the dimensionless scale as a first step. One generally reduces the volume of parameters and remove physical units from the system, which will facilitate mathematical investigations and make the model more flexible for experimentalists who wish to implement the system *in vivo* or *in vitro* as the units are not specified. By using the scaling $\overline{\omega_j} = \frac{\omega_j}{K_\omega}$, $\overline{r_j} = \frac{r_j}{K_r}$,

Preprints (www.preprints.org) | NOT PEER-REVIEWED | Posted: 7 July 2022 doi:10.20944/preprints202207.0110.v1

$\overline{p} = \frac{p}{K_p}$, $\overline{t} = \delta_p t$, $\overline{u_j} = k u_j$, the dimensionless model becomes (overlines have been dropped for simplicity.):

$$\begin{cases} \frac{dp}{dt} = \sum_{j=1}^{N} \alpha \left(\frac{\omega_j^a}{1+\omega_j^a} \right) \left(\frac{1}{1+r_j^b} \right) - p \\ \frac{d\omega_j}{dt} = \beta \left(\frac{p^b}{1+p^b} \right) \left(\frac{1}{1+r_j^b} \right) - \theta \omega_j + \tau_j \\ r_j = \frac{S}{1+u_j} \end{cases} \tag{2}$$

where $\alpha = \frac{v_p}{K_p \delta_p}$, $\beta = \frac{v_\omega}{K_\omega \delta_p}$, $\theta = \frac{\delta_\omega}{\delta_p}$, $\tau_j = \frac{\epsilon_j}{K_\omega \delta_p}$, $S = \frac{R}{K_r}$.

Now we try to intuitively interpret whether the reinforcement effect can be realized by the Fernando's model or not. Suppose we carry out the conditioning twice, in order to guarantee that the second learned response is more abundant than the first one, the simplest way is to ensure that the initial concentration of ω_2 is small and the growth parameter β is not too large so that we can anticipate p to keep growing with the repeated conditioning according to Equation 2. Next we investigate how the two stimuli dissociate. Intuitively, in light of the design of the Fernando's model, the disappearance of the learned response is dictated by the time elapse. This is due to the fact that ω_2 promotes the production of p such that the response will eventually disappear only if ω_2 falls to 0. Additionally, the learned response will not attenuate if the time interval between two successive stimuli is insufficient relative to the decay rate. In all, the dissociation is autonomous and is not dictated by the repeated cuing of the conditioned stimulus (alone). This can be circumvented by a different design which will be introduced next.

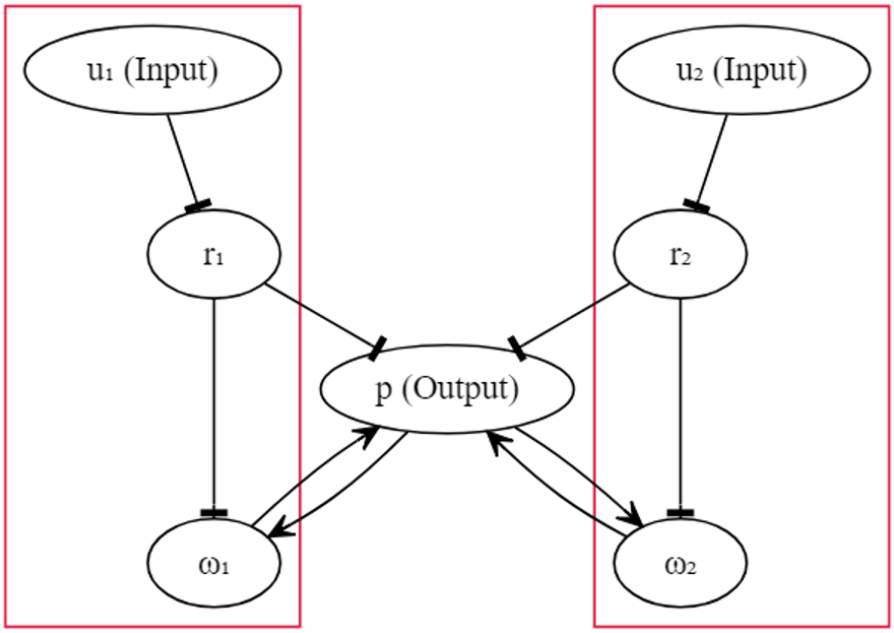

Figure 1. The schematic circuit of the Fernando's model.

2.2. *A model with forced dissociation*

The circuit for the model proposed here is inspired by the work [18] and is shown in Figure 2. In the diagram, each oval box denotes a particular protein molecule and we again omit the genes for the illustrative brevity. More specifically, input x initiates the transcription of a particular gene which guides the manufacturing of molecule u; the translation of molecule v is controlled by another gene, the expression of which is dictated by x, u and z all together; Similarly, y is controlled by a third gene, the expression of which is dictated by x, v and z. The activation is drawn with an arrow and the inhibition is drawn

Preprints (www.preprints.org) | NOT PEER-REVIEWED | Posted: 7 July 2022 doi:10.20944/preprints202207.0110.v1

with a hammerhead. Input x plays the role of the conditioned stimulus, input z plays the role of unconditioned stimulus and y represents the response. However, we do need to point out here that the discrimination between the conditioned and unconditioned stimulus has been downplayed in some sense and we will explain this in the discussion part. The design of this new architecture comes with at least two purposes. First of all, we intend to construct a simple circuit of which the mechanism is completely different from the Fernando's model. We hope the components of the circuit are more interactive with each other and the association is not reliant upon the participation of the feedback loops. These may lift a few restrictions on the synthetic implementation. Secondly, given that the Fernando's model is not capable of demonstrating forced dissociation, we hope to build a model that can successfully dissociate the two stimuli by repeating the cuing of the conditioned stimulus alone right after the conditioning. To fulfill the latter requirement, instead of placing a molecule (ω_2 in the Fernando's model) that promotes the transcription of the response protein molecule, we can actually consider introducing an inhibitor upstream of the response molecule. In this way, the consistent input of conditioned stimulus alone is expected to reduce the amount of the response molecule, so long as the stimulus promotes the expression of the inhibitor after the conditioning of conditioned and unconditioned stimulus. This explains why we introduce the $x \to v \to y$ pathway in Figure 2. As for the other parts of the circuit, $z \to y$ and $z \to v \to y$ guarantee that input z can always activate the output y, $x \to y$ ensures that there can exist sufficient amount of learned response upon formation of associative learning, and u works as a moderator speeding up the consumption of v that makes the reinforcement effect more likely to occur. Here we assume the Hill coefficients for all molecules are identical and are denoted by a.

By employing the Hill equation, the system can be described by the following equations:

$$\begin{cases} \dfrac{dy}{dt} = \alpha_{yx}\left(\dfrac{x^a}{K_x^a + x^a}\right)\left(\dfrac{K_z^a}{K_z^a + z^a}\right)\left(\dfrac{K_v^a}{K_v^a + v^a}\right) \\ \quad + \alpha_{yz}\left(\dfrac{K_x^a}{K_x^a + x^a}\right)\left(\dfrac{z^a}{K_z^a + z^a}\right)\left(\dfrac{K_v^a}{K_v^a + v^a}\right) \\ \quad + \alpha_{xyz}\left(\dfrac{x^a}{K_x^a + x^a}\right)\left(\dfrac{z^a}{K_z^a + z^a}\right)\left(\dfrac{K_v^a}{K_v^a + v^a}\right) \\ \quad - \delta_y y \\ \dfrac{du}{dt} = \alpha_{ux}\dfrac{x^a}{K_x^a + x^a} - \delta_u u \\ \dfrac{dv}{dt} = \alpha_{vx}\left(\dfrac{x^a}{K_x^a + x^a}\right)\left(\dfrac{K_u^a}{K_u^a + u^a}\right)\left(\dfrac{K_z^a}{K_z^a + z^a}\right) - \delta_v v \end{cases} \tag{3}$$

Similarly to the Fernando's model, here K_x, K_z, K_v and K_u denote the respective Hill constants for molecule x, z, v and u. The production and degradation rate are denoted by α and δ where the subscripts are used to signify the source of contribution. Then we use a similar scaling approach to make the system dimensionless. The dimensionless system is shown as below:

$$\begin{cases} \dfrac{dy}{dt} = \alpha_{yx}\left(\dfrac{x^a}{1 + x^a}\right)\left(\dfrac{1}{1 + z^a}\right)\left(\dfrac{1}{1 + v^a}\right) \\ \quad + \alpha_{yz}\left(\dfrac{1}{1 + x^a}\right)\left(\dfrac{z^a}{1 + z^a}\right)\left(\dfrac{1}{1 + v^a}\right) \\ \quad + \alpha_{xyz}\left(\dfrac{x^a}{1 + x^a}\right)\left(\dfrac{z^a}{1 + z^a}\right)\left(\dfrac{1}{1 + v^a}\right) \\ \quad - y \\ \dfrac{du}{dt} = \alpha_{ux}\dfrac{x^a}{1 + x^a} - \beta_u u \\ \dfrac{dv}{dt} = \alpha_{vx}\left(\dfrac{x^a}{1 + x^a}\right)\left(\dfrac{1}{1 + u^a}\right)\left(\dfrac{1}{1 + z^a}\right) - \beta_v v \end{cases} \tag{4}$$

Preprints (www.preprints.org) | NOT PEER-REVIEWED | Posted: 7 July 2022 doi:10.20944/preprints202207.0110.v1

One of the drawbacks of this circuit, one may have already noted, is that the model is not as heuristic as the Fernando's model. Indeed, the Fernando's model borrows the architecture of Hebbian learning whereas we built our model from scratch tailored for the properties we want to achieve. Intuitively, in order to make the reinforcement effect occur, we anticipate that by properly choosing the parameter values, the presence of x alone can significantly elevate the amount of v and the conditioning (whenever both x and z are present) can speed up the consumption of v. This will ensure that the second learned response is more abundant than the first one and at the same time, the response to the conditioned stimulus alone is less abundant than to the unconditioned stimulus. When it comes to forced dissociation, as we discussed previously, repeated cuing of input x alone after the conditioning can elevate the concentration of v which subsequently reduces the output y as a result of $x \to v \to y$. The numerical result will be given in the next section.

Before closing this section, we would want to briefly mention a potential adjustment to the current circuit that can simplify the system given in Equation 4. Our existing scheme allows for x, v and z to bind at a single operator site. In fact, we can adjust the output part in a way such that z exploits operator sites that only restrict to z itself, which makes it look somehow analogous to the output part of the Fernando's model in which the left half and the right half are unrelated. The dimensionless model arising from the adjustment can then be reduced to:

$$\begin{cases} \dfrac{dy}{dt} = \alpha_{yx}\left(\dfrac{x^a}{1+x^a}\right)\left(\dfrac{1}{1+v^a}\right) + \alpha_{yz}\left(\dfrac{z^a}{1+z^a}\right) - y \\ \dfrac{du}{dt} = \alpha_{ux}\dfrac{x^a}{1+x^a} - \beta_u u \\ \dfrac{dv}{dt} = \alpha_{vx}\left(\dfrac{x^a}{1+x^a}\right)\left(\dfrac{1}{1+u^a}\right)\left(\dfrac{1}{1+z^a}\right) - \beta_v v \end{cases} \tag{5}$$

The adjustment provides an alternative with a simpler mathematical formulation (but likely with more biological complexity) for readers who wish to implement our circuit. We will later demonstrate that this adjusted model can also display the same qualitative behaviors.

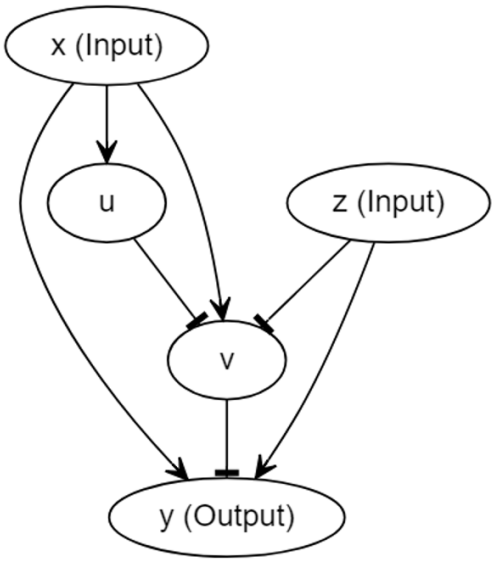

Figure 2. The schematic circuit of the model with forced dissociation.

3. Results

The numerical simulations were conducted in MATLAB R2020b. As the ODE systems are too complex to be analyzed in terms of the numerical stability [64,65], we first used the Runge–Kutta 4th order method [66] to obtain a benchmark result for the models and for the purpose of efficiency, we used the forward Euler method with time step $\Delta t = 0.01$ to carry

 doi:10.20944/preprints202207.0110.v1

out the entire analysis. We gradually reduced the time step from $\Delta t = 0.1$ and the result remains unchanged, which demonstrates that the numerical method is stable in this case.

Figure 7(a) displays one simulation result for the Fernando's model (Equation 2) and the parameter values used in the simulation are listed in Table 1. Here we use the Hill coefficients recommended in [60], which are $a = 4$ and $b = 2$.

The first spike in p is stimulated by the unconditioned stimulus u_1. The second (small) spike in response p is triggered by the conditioned stimulus u_2. Of course, the response p can be retained to 0 only in the presence of u_2 by setting the initial concentration of ω_2 to 0 just like the authors did in the original paper, but here we want to highlight the fact that various levels of conditioned response are available to choose. The first conditioning is formed at the third spike and the second conditioning is formed at the fifth spike in p when both u_1 and u_2 are present. The fourth and the sixth spike in p represent the first and the second learned response respectively when solely u_2 is present. As can be seen, the learned response has been reinforced after the repeated conditioning. Next, we move on to the discussion of how the two stimuli dissociate, namely, how the learned response is attenuated in the presence of consecutive conditioned stimulus alone after the formation of conditioning. The conjecture made in the previous section is validated by the last four spikes in response p in Figure 7(a). As is apparent, the sixth, seventh and the eighth spike are of the same amplitude as the time intervals are not wide enough. Conversely, the response starts to decrease (shown by the last two spikes) when the time interval is further widened. This can be deemed a limitation for the model because in some applications (e.g., immune inflammation), we may hope to force the stimuli to dissociate by repeated cuing of the conditioned stimulus alone in a short time window, after the formation of associative learning, which forms one of the motivations for our novel design.

Furthermore, we would also like to study whether the qualitative behaviors of associative learning that we introduced previously are preserved or not apart from using the Hill coefficients recommended in [60]. The values for the other parameters will remain the same as shown in Table 1.

First, we fix $b = 2$ and alter the Hill coefficient for the weight molecules from $a = 1$ to $a = 4$. The respective responses of molecule p are displayed in Figure 3. As is obvious from the figure, The qualitative behaviors have barely changed irrespective of the value of a apart from the fact the $a = 1$ gives rise to a relatively notable response when only the conditioned stimulus u_2 is present prior to conditioning. However, the result of $a = 1$ can still be classified as a valid associative learning in broad term as the response triggered by the conditioned stimulus u_2 alone is more significant after conditioning than before.

Then we study the case when $a = b$ and we alter a from $a = 1$ to $a = 4$. The respective responses of molecule p are displayed in Figure 4. As can be seen from the figure, only $a = 1$ gives rise to undesirable behaviors as the concentration of response p never comes down to 0. This is because $a = 1$ leads to a large transient growth rate of the weight for the conditioned stimulus ω_2.

In all, the Fernando's model is robust to the variation of the Hill coefficients even without exploring the other parameters. It may offer more flexibility to synthetic biologists since one doesn't have to require two dimers to be bound cooperatively for weight molecule ω_1 and ω_2. As we have shown in Figure 3, even $a = 1$ and $b = 2$ can produce desirable results, which may reduce the experimental complexity.

Preprints (www.preprints.org) | NOT PEER-REVIEWED | Posted: 7 July 2022 doi:10.20944/preprints202207.0110.v1

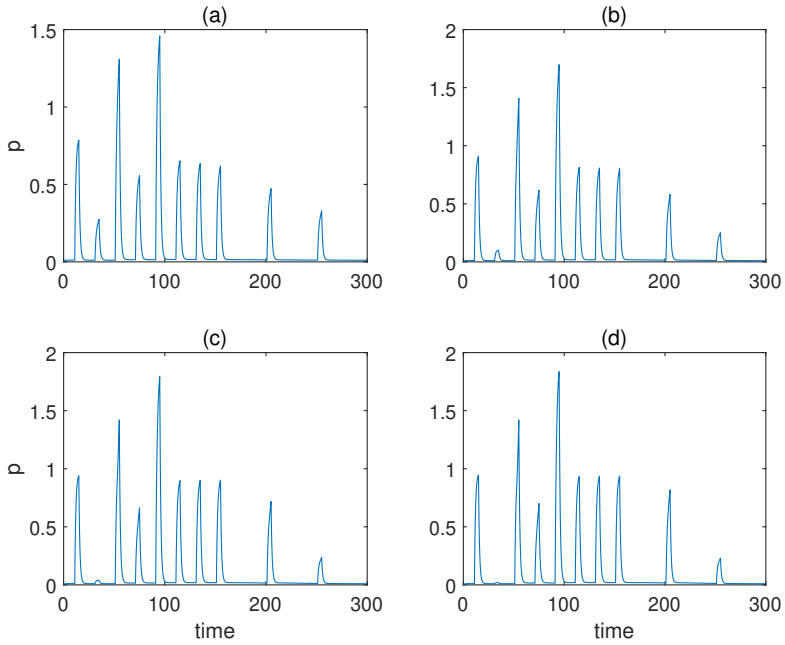

Figure 3. The concentration of molecule p under various Hill coefficient a when the value of b is fixed for the Fernando's model. From (a) to (d) display the results when $a = 1, 2, 3, 4$. $b = 2, \alpha = 1, \beta = 0.8, \theta = 0.02, \tau = 0.1, S = 10$.

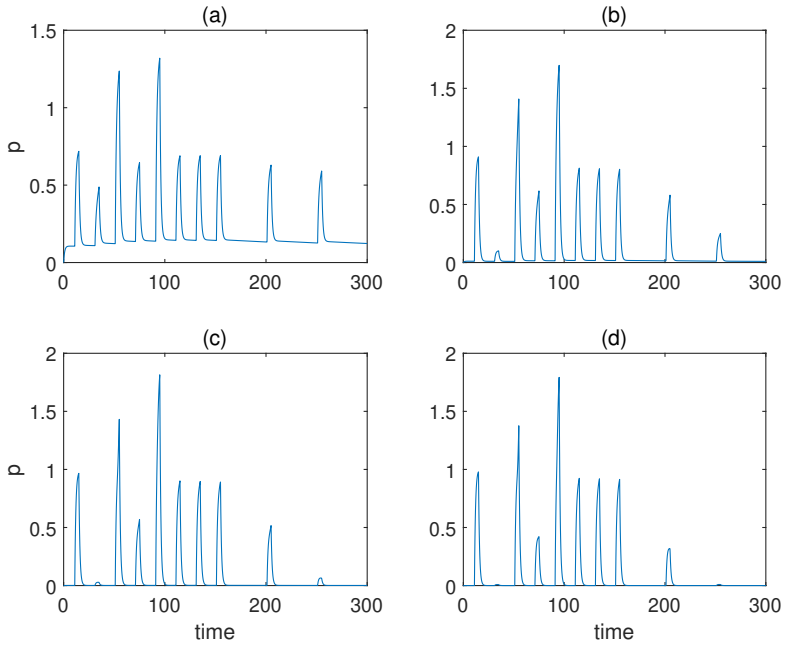

Figure 4. The concentration of molecule p under various Hill coefficient when $a = b$ for the Fernando's model. From (a) to (d) display the results when $a = 1, 2, 3, 4$. $\alpha = 1, \beta = 0.8, \theta = 0.02, \tau = 0.1, S = 10$.

 doi:10.20944/preprints202207.0110.v1

Table 1: Parameter values used in the simulation for the Fernando's model (Equation 2).

Parameter	Value
α	1
β	0.8
θ	0.02
τ	0.1
S	10

Figure 7(b) displays the simulation result for the model with forced dissociation (Equation 4) using $a = 2$ and the other parameter values used in the simulation are listed in Table 2.

The first spike in response y is stimulated by the unconditioned stimulus z and the second spike is stimulated by the conditioned stimulus x. The first conditioning is formed at the third spike and the second conditioning is formed at the fifth spike in p when both z and x are present. The fourth and the sixth spike in p represent the first and the second learned response respectively. As can be seen, the learned response has been reinforced after the repeated conditioning. As opposed to the Fernando's model, this model can successfully repress the learned response to the preconditioned level by means of repeated cuing of the conditioned stimulus within a short time window, which has been corroborated by the last two spikes in response y in Figure 7(b).

Considering our model is not as heuristic as the Fernando's model, it is necessary to validate that the reinforcement effect is indeed the result of the conditioning. Therefore, we remove the second and the third unconditioned stimulus z from the system and the result is shown in Figure 8(a). As can be seen, the reinforcement effect no longer exists without the the conditioning of x and z. The result also validates our conjecture in the previous section that the presence of x as well as z speeds up the degradation of u, which is the game changer for the formation of reinforcement effect.

Similarly to what we have done for the Fernando's model, we will study the behaviors of this model under various Hill coefficient a with the other parameters specified in Table 2 unchanged.

From $a = 1$ to $a = 4$, the respective responses of molecule y are displayed in Figure 5. As can be observed, only $a = 2$ and $a = 3$ yield desirable associative learning behaviors. The effect of conditioning is not discriminative for $a = 1$, and for $a = 4$, the response during condition is not more significant than the one when only unconditioned stimulus is present.

The adjusted model (Equation 5) introduced previously can also display the qualitative behaviors which are shown in Figure 8(b) when using $a = 2$. The parameter values used in this simulation are listed in Table 3. What is worth noticing is that the adjusted model can give rise to more abundant response on the dimensionless scale, as compared to the original version (Figure 7(b) and Figure 8(b)).

Again, we study the behaviors of the model with various Hill coefficient a without changing the other parameters specified in Table 3. As is apparent from Figure 6, the qualitative behaviors of the associative learning have been largely preserved. However, the learned responses for the case $a = 3$ and $a = 4$ are less significant as compared to $a = 2$.

Preprints (www.preprints.org) | NOT PEER-REVIEWED | Posted: 7 July 2022 doi:10.20944/preprints202207.0110.v1

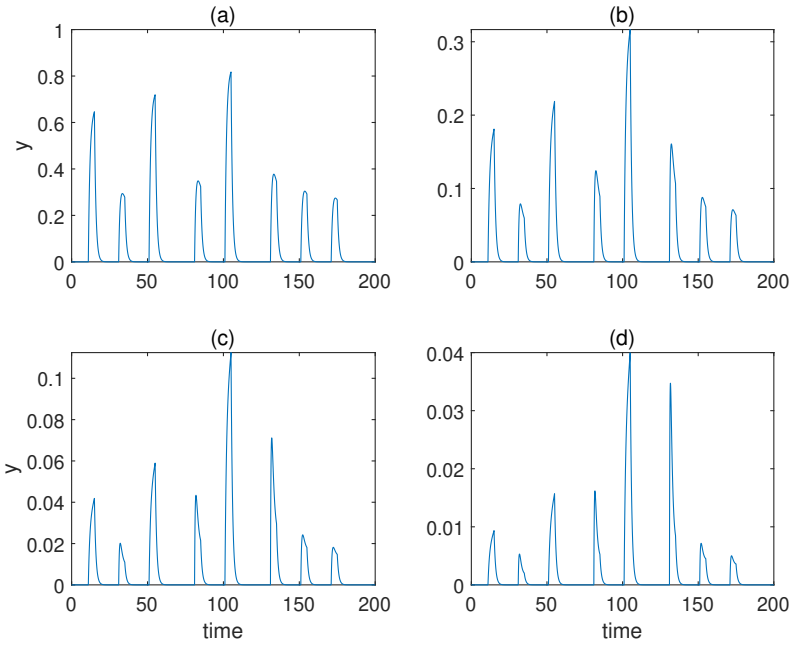

Figure 5. The concentration of molecule y under various Hill coefficient a for the model with forced dissociation. From (a) to (d) display the results when $a = 1, 2, 3, 4$. $\alpha_{yx} = 2, \alpha_{yz} = 4, \alpha_{xyz} = 4, \alpha_{ux} = 0.6, \alpha_{vx} = 1.5, \beta_u = 0.1, \beta_v = 0.02$.

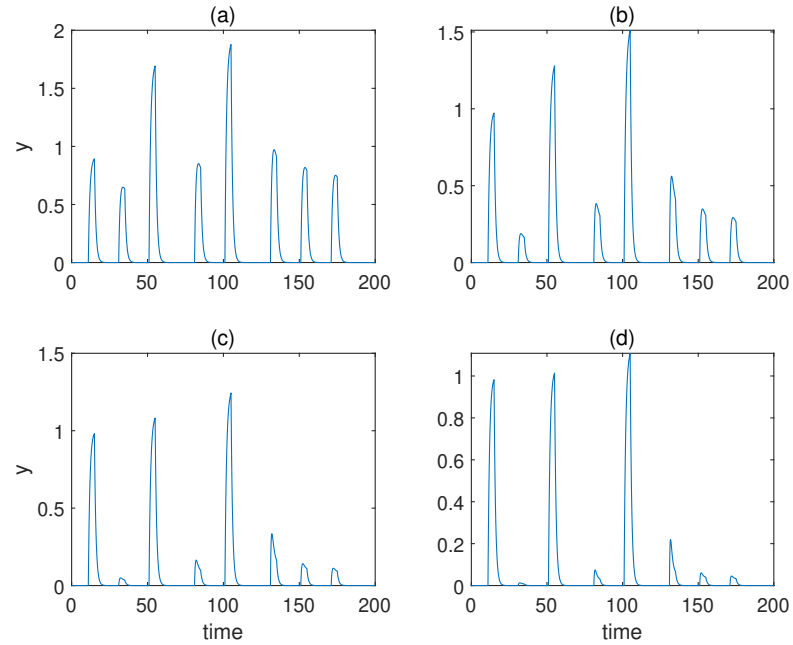

Figure 6. The concentration of molecule y under various Hill coefficient a for the adjusted model with forced dissociation. From (a) to (d) display the results when $a = 1, 2, 3, 4$. $\alpha_{yx} = 4, \alpha_{yz} = 1, \alpha_{ux} = 0.6, \alpha_{vx} = 1, \beta_u = 0.1, \beta_v = 0.02$.

 doi:10.20944/preprints202207.0110.v1

Table 2: Parameter values used in the simulation for the model with forced dissociation (Equation 4).

Parameter	Value
α_{yx}	2
α_{yz}	4
α_{xyz}	4
α_{ux}	0.6
α_{vx}	1.5
β_u	0.1
β_v	0.02

Table 3: Parameter values used in the simulation for the adjusted model with forced dissociation (Equation 5).

Parameter	Value
α_{yx}	4
α_{yz}	1
α_{ux}	0.6
α_{vx}	1
β_u	0.1
β_v	0.02

Preprints (www.preprints.org) | NOT PEER-REVIEWED | Posted: 7 July 2022 doi:10.20944/preprints202207.0110.v1

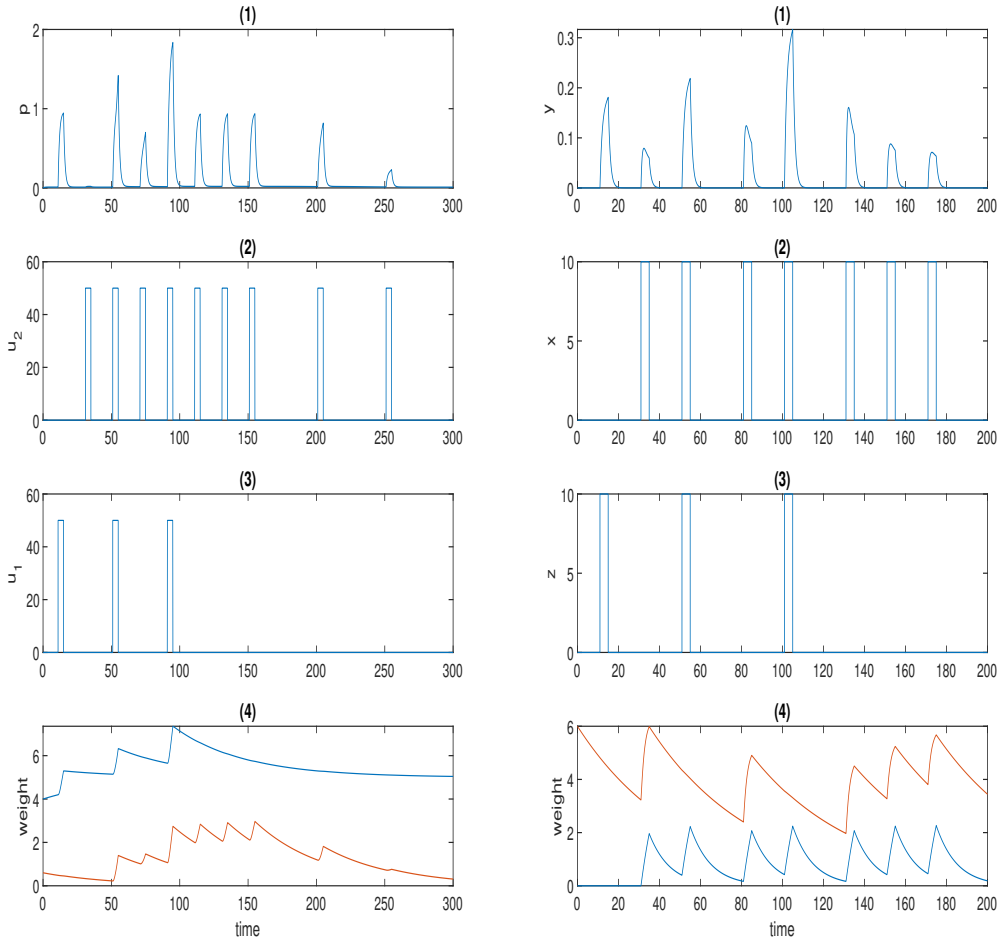

(a) (b)

Figure 7. (a) Time series for the Fernando's model: (1) response molecule p; (2), (3) conditioned stimulus u_2 and unconditioned stimulus u_1; (4) weight molecule ω_1 (blue) and ω_2 (red); $\alpha = 1, \beta = 0.8, \theta = 0.02, \tau = 0.1, S = 10$. (b): Time series for the model with forced dissociation (1) response molecule y; (2), (3) conditioned stimulus x and unconditioned stimulus z; (4) weight molecule u (blue) and v (red); $a = 2, \alpha_{yx} = 2, \alpha_{yz} = 4, \alpha_{xyz} = 4, \alpha_{ux} = 0.6, \alpha_{vx} = 1.5, \beta_u = 0.1, \beta_v = 0.02$. In (1), the first spike is stimulated by the unconditioned stimulus and the second spike is triggered by the conditioned stimulus; the first and the second conditioning are formed at the third and the fifth spike respectively; the first and the second learned response are reflected by the fourth and the sixth spike; the remaining spikes demonstrate whether the forced dissociation can be realized or not.

Preprints (www.preprints.org) | NOT PEER-REVIEWED | Posted: 7 July 2022 doi:10.20944/preprints202207.0110.v1

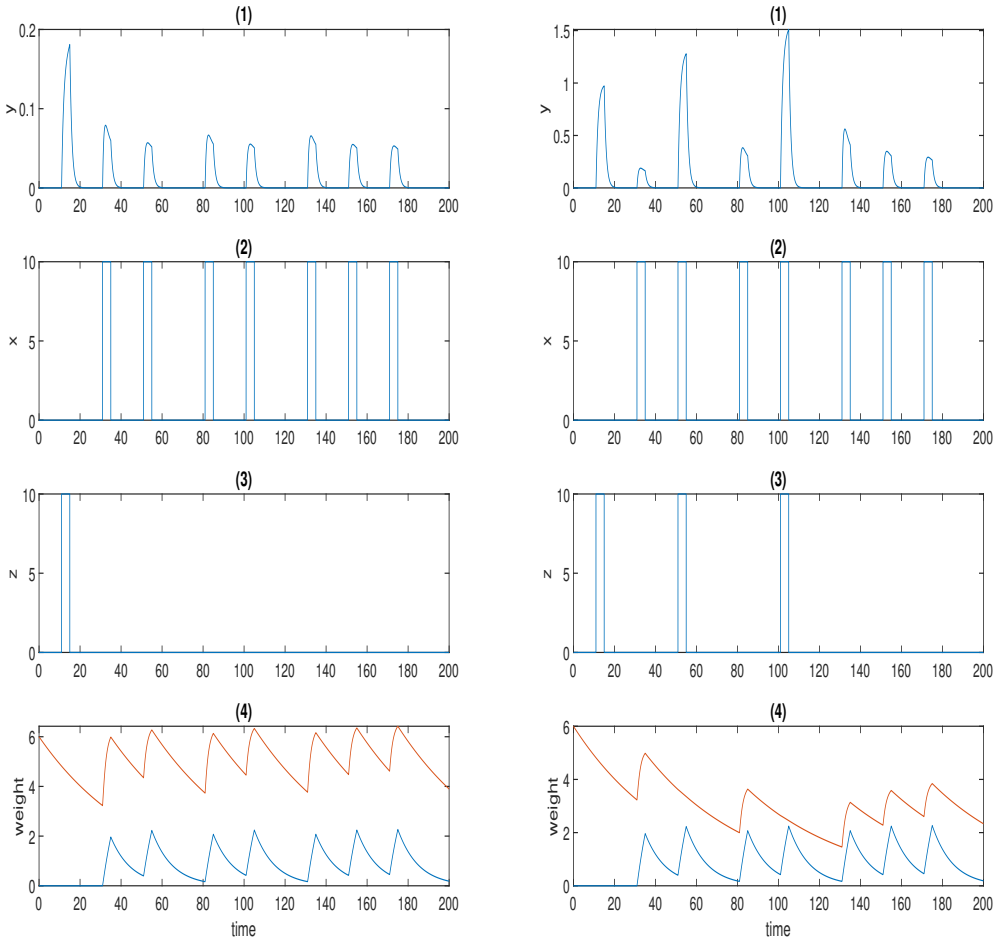

(a) (b)

Figure 8. (a): Time series for the model with forced dissociation without conditioning (1) response molecule y; (2), (3) conditioned stimulus x and unconditioned stimulus z; (4) weight molecule u (blue) and v (red); $a = 2, \alpha_{yx} = 2, \alpha_{yz} = 4, \alpha_{xyz} = 4, \alpha_{ux} = 0.6, \alpha_{vx} = 1.5, \beta_u = 0.1, \beta_v = 0.02$. (b): Time series for the adjusted model with forced dissociation (1) response molecule y; (2), (3) conditioned stimulus x and unconditioned stimulus z; (4) weight molecule u (blue) and v (red); $a = 2, \alpha_{yx} = 4, \alpha_{yz} = 1, \alpha_{ux} = 0.6, \alpha_{vx} = 1, \beta_u = 0.1, \beta_v = 0.02$.

4. Discussion

In this work, we presented a detailed analysis of two advanced behaviors (reinforcement effect and forced dissociation) in associative learning. The Fernando's model can successfully demonstrate reinforcement effect if we properly choose the parameter values. However, the attenuation of learned response only occurs when the time interval between learned response is big enough, in the sense that there is no way to force the learned response to decrease within a short time window. The model introduced in Chapter 2.2 has been shown to be able to manifest reinforcement effect as well as forced dissociation with the parameter values listed in Table 2, which can potentially provide more possibilities for the biological and medical applications of synthetic biology.

Having highlighted the contribution of our model, we must point out that it comes with a few constraints that synthetic biologists need to be aware of. First of all, the overall qualitative behavior of the system is not very robust to the parameters aside from the Hill coefficients. We found that a 25% change in parameter values could lead to less desirable

Preprints (www.preprints.org) | NOT PEER-REVIEWED | Posted: 7 July 2022 doi:10.20944/preprints202207.0110.v1

behaviors. An example is given in Figure 9 where α_{ux} has been changed from 0.6 to 0.45. The first spike is now of the same amplitude as the third in response y. But the stringent constraint can be relaxed if we only expect to implement only one of the two behaviors, either reinforcement effect or forced dissociation. Secondly, it is extremely difficult, if not impossible, to control the response to the conditioned stimulus prior to conditioning at an insignificant level (second spike in y in Figure 7(b)), while maintaining the behaviors of interest. Hence, the model proposed here may not be a suitable candidate to emulate the behaviors of Pavlov's dog, but fits the context of associative learning in a broader sense where the conditioning and learning are of the major concern. Thirdly, the model demands that v remains abundant in order for the associative learning to happen. Therefore, v needs to be supplemented to a sufficient level before the start of each experiment. Otherwise, the conditioned stimulus x alone could result in an over-expression of the response.

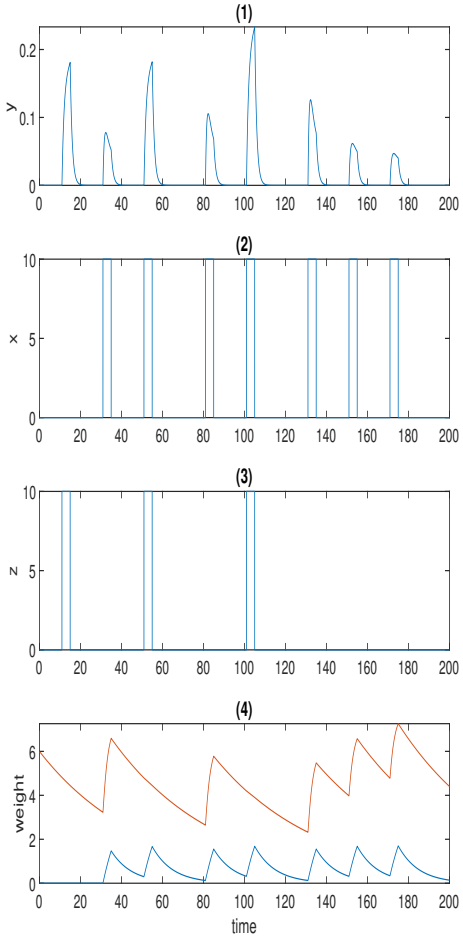

Figure 9. An example to illustrate the effect of change in parameter values on the model with forced dissociation. $a = 2, \alpha_{yx} = 2, \alpha_{yz} = 4, \alpha_{xyz} = 4, \alpha_{ux} = 0.45, \alpha_{vx} = 1.5, \beta_u = 0.1, \beta_v = 0.02$.

Last but not least, we also want to mention several potential applications of our work in the field of synthetic biology and medicine. Firstly, for the treatment for diabetes: Ye *et al*. [67] built a synthetic signaling cascade that enhances blood-glucose homeostasis. The reinforcement effect we demonstrated in the models may pave the way for further adjustment to the circuit in the hope to attain more efficient control of glucose level. Secondly, for the treatment for immune-mediated disease, the adoptive T-cell transfer technology has shown immense promise in the treatment of immune-mediated disease

such as cancer immunotherapy [68]. The feature of forced dissociation displayed in our model may provide more flexibility for experimentalists to shut off the excessive immune response once the tumors are eliminated. Finally, some recent studies have been focused on modeling the network of neurodegenerative markers [69,70]. The models we discussed in this article may shed light on how to model these new findings at the genetic circuit level and build hierarchical neuronal architectures. Besides, the models may play a supportive role in the existing technology that controls neurotransmitter release [71].

Author Contributions: Supervision: AZ; conceptualization: AZ and ZL; model derivation: AF and ZL; numerical simulation: ZL; writing: ZL, AZ, AF and PT.

Funding: This project is funded by CRUK Early Detection Committee Project Award C12077/A26223.

Institutional Review Board Statement: Not applicable

Informed Consent Statement: Not applicable

Acknowledgments: Medical Research Council grant (MR/R02524X/1) is acknowledged by AZ, the Russian Science Foundation Grant No 22-12-00216 by AZ, and CRUK Early Detection Committee Project Award C12077/A26223 by ZL and AZ.

Conflicts of Interest: The authors declare no conflict of interest.

References

1. Benner SA, Sismour AM. Synthetic biology. Nature Reviews Genetics. 2005 Jul;6(7):533-43.
2. Cameron DE, Bashor CJ, Collins JJ. A brief history of synthetic biology. Nature Reviews Microbiology. 2014 May;12(5):381-90.
3. Khalil AS, Collins JJ. Synthetic biology: applications come of age. Nature Reviews Genetics. 2010 May;11(5):367-79.
4. Ruder WC, Lu T, Collins JJ. Synthetic biology moving into the clinic. Science. 2011 Sep 2;333(6047):1248-52.
5. Bueso YF, Lehouritis P, Tangney M. In situ biomolecule production by bacteria; a synthetic biology approach to medicine. Journal of Controlled Release. 2018 Apr 10;275:217-28.
6. Wu MR, Jusiak B, Lu TK. Engineering advanced cancer therapies with synthetic biology. Nature Reviews Cancer. 2019 Apr;19(4):187-95.
7. Goold HD, Wright P, Hailstones D. Emerging opportunities for synthetic biology in agriculture. Genes. 2018 Jul;9(7):341.
8. Wurtzel ET, Vickers CE, Hanson AD, Millar AH, Cooper M, Voss-Fels KP, Nikel PI, Erb TJ. Revolutionizing agriculture with synthetic biology. Nature Plants. 2019 Dec;5(12):1207-10.
9. Ke J, Wang B, Yoshikuni Y. Microbiome engineering: synthetic biology of plant-associated microbiomes in sustainable agriculture. Trends in biotechnology. 2021 Mar 1;39(3):244-61.
10. Bueso YF, Tangney M. Synthetic biology in the driving seat of the bioeconomy. Trends in biotechnology. 2017 May 1;35(5):373-8.
11. Anderson JC, Clarke EJ, Arkin AP, Voigt CA. Environmentally controlled invasion of cancer cells by engineered bacteria. Journal of molecular biology. 2006 Jan 27;355(4):619-27.
12. Jinek M, Chylinski K, Fonfara I, Hauer M, Doudna JA, Charpentier E. A programmable dual-RNA–guided DNA endonuclease in adaptive bacterial immunity. science. 2012 Aug 17;337(6096):816-21.
13. Xu X, Qi LS. A CRISPR–dCas toolbox for genetic engineering and synthetic biology. Journal of molecular biology. 2019 Jan 4;431(1):34-47.
14. Ren J, Lee J, Na D. Recent advances in genetic engineering tools based on synthetic biology. Journal of Microbiology. 2020 Jan;58(1):1-0.
15. Jensen MK, Keasling JD. Recent applications of synthetic biology tools for yeast metabolic engineering. FEMS Yeast Res. 2015 Feb 1;15(1):1-0.
16. Hughes RA, Ellington AD. Synthetic DNA synthesis and assembly: putting the synthetic in synthetic biology. Cold Spring Harbor perspectives in biology. 2017 Jan 1;9(1):a023812.
17. Borg Y, Grigonyte AM, Boeing P, Wolfenden B, Smith P, Beaufoy W, Rose S, Ratisai T, Zaikin A, Nesbeth DN. Open source approaches to establishing Roseobacter clade bacteria as synthetic biology chassis for biogeoengineering. PeerJ. 2016 Jul 7;4:e2031.
18. Nesbeth DN, Zaikin A, Saka Y, Romano MC, Giuraniuc CV, Kanakov O, Laptyeva T. Synthetic biology routes to bio-artificial intelligence. Essays in biochemistry. 2016 Nov 30;60(4):381-91.
19. Bianchini F. Artificial intelligence and synthetic biology: a tri-temporal contribution. Biosystems. 2016 Oct 1;148:32-9.
20. Abrego L, Zaikin A. Integrated information as a measure of cognitive processes in coupled genetic repressilators. Entropy. 2019 Apr;21(4):382.
21. Yang J, Lee J, Land MA, Lai S, Igoshin OA, St-Pierre F. A synthetic circuit for buffering gene dosage variation between individual mammalian cells. Nature communications. 2021 Jul 5;12(1):1-3.
22. Kim J, White KS, Winfree E. Construction of an in vitro bistable circuit from synthetic transcriptional switches. Molecular systems biology. 2006;2(1):68.

23. Bacchus W, Aubel D, Fussenegger M. Biomedically relevant circuit-design strategies in mammalian synthetic biology. Molecular systems biology. 2013;9(1):691.
24. Brophy JA, Voigt CA. Principles of genetic circuit design. Nature methods. 2014 May;11(5):508-20.
25. Kobayashi H, Kaern M, Araki M, Chung K, Gardner TS, Cantor CR, Collins JJ. Programmable cells: interfacing natural and engineered gene networks. Proceedings of the National Academy of Sciences. 2004 Jun 1;101(22):8414-9.
26. Xie M, Fussenegger M. Designing cell function: assembly of synthetic gene circuits for cell biology applications. Nature Reviews Molecular Cell Biology. 2018 Aug;19(8):507-25.
27. Xia PF, Ling H, Foo JL, Chang MW. Synthetic genetic circuits for programmable biological functionalities. Biotechnology advances. 2019 Nov 1;37(6):107393.
28. Tolle F, Stücheli P, Fussenegger M. Genetic circuitry for personalized human cell therapy. Current opinion in biotechnology. 2019 Oct 1;59:31-8.
29. Prochazka L, Benenson Y, Zandstra PW. Synthetic gene circuits and cellular decision-making in human pluripotent stem cells. Current Opinion in Systems Biology. 2017 Oct 1;5:93-103.
30. Nene NR, Garca-Ojalvo J, Zaikin A. Speed-dependent cellular decision making in nonequilibrium genetic circuits. PloS one. 2012 Mar 13;7(3):e32779.
31. Filicheva S, Zaikin A, Kanakov O. Dynamical decision making in a genetic perceptron. Physica D: Nonlinear Phenomena. 2016 Apr 1;318:112-5.
32. Abrego L, Zaikin A. Decision making in an intracellular genetic classifier. Mathematical Modelling of Natural Phenomena. 2017;12(4):30-42.
33. Kanakov O, Kotelnikov R, Alsaedi A, Tsimring L, Huerta R, Zaikin A, Ivanchenko M. Multi-input distributed classifiers for synthetic genetic circuits. PLoS One. 2015 May 6;10(5):e0125144.
34. Macia J, Vidiella B, Solé RV. Synthetic associative learning in engineered multicellular consortia. Journal of The Royal Society Interface. 2017 Apr 30;14(129):20170158.
35. Borg Y, Alsford S, Pavlika V, Zaikin A, Nesbeth DN. Synthetic biology tools for engineering Goodwin oscillation in Trypanosoma brucei brucei. Heliyon. 2022 Feb 1;8(2):e08891.
36. Ullner E, Koseska A, Zaikin A, Volkov E, Kurths J, Garcia-Ojalvo J. Dynamics of multicellular synthetic gene networks. Handbook on Biological Networks, World Scientific, Singapore. 2009 Dec 4.
37. Ullner E, Ares S, Morelli LG, Oates AC, Jülicher F, Nicola E, Heussen R, Whitmore D, Blyuss K, Fryett M, Zakharova A. Noise and oscillations in biological systems: Multidisciplinary approach between experimental biology, theoretical modelling and synthetic biology. International Journal of Modern Physics B. 2012 Oct 10;26(25):1246009.
38. Ullner E, Zaikin A, Volkov EI, García-Ojalvo J. Multistability and clustering in a population of synthetic genetic oscillators via phase-repulsive cell-to-cell communication. Physical review letters. 2007 Oct 2;99(14):148103.
39. Anesiadis N, Kobayashi H, Cluett WR, Mahadevan R. Analysis and design of a genetic circuit for dynamic metabolic engineering. ACS synthetic biology. 2013 Aug 16;2(8):442-52.
40. Shanks DR. The psychology of associative learning. Cambridge University Press; 1995.
41. Wasserman EA, Miller RR. What's elementary about associative learning?. Annual review of psychology. 1997 Feb;48(1):573-607.
42. Pearce JM, Bouton ME. Theories of associative learning in animals. Annual review of psychology. 2001 Feb;52(1):111-39.
43. Behrens TE, Hunt LT, Woolrich MW, Rushworth MF. Associative learning of social value. Nature. 2008 Nov;456(7219):245-9.
44. Mitchell CJ, De Houwer J, Lovibond PF. The propositional nature of human associative learning. Behavioral and Brain Sciences. 2009 Apr;32(2):183-98.
45. Pavlov PI. Conditioned reflexes: an investigation of the physiological activity of the cerebral cortex. Annals of neurosciences. 2010 Jul;17(3):136.
46. Ziegler M, Soni R, Patelczyk T, Ignatov M, Bartsch T, Meuffels P, Kohlstedt H. An electronic version of Pavlov's dog. Advanced Functional Materials. 2012 Jul 10;22(13):2744-9.
47. Fanselow MS, Poulos AM. The neuroscience of mammalian associative learning. Annu. Rev. Psychol.. 2005 Feb 4;56:207-34.
48. Uwano T, Nishijo H, Ono T, Tamura R. Neuronal responsiveness to various sensory stimuli, and associative learning in the rat amygdala. Neuroscience. 1995 Sep 1;68(2):339-61.
49. Faber T, Joerges J, Menzel R. Associative learning modifies neural representations of odors in the insect brain. Nature neuroscience. 1999 Jan;2(1):74-8.
50. Johansen JP, Diaz-Mataix L, Hamanaka H, Ozawa T, Ycu E, Koivumaa J, Kumar A, Hou M, Deisseroth K, Boyden ES, LeDoux JE. Hebbian and neuromodulatory mechanisms interact to trigger associative memory formation. Proceedings of the National Academy of Sciences. 2014 Dec 23;111(51):E5584-92.
51. Bray D. Molecular networks: the top-down view. Science. 2003 Sep 26;301(5641):1864-5.
52. Jacob EB, Becker I, Shapira Y, Levine H. Bacterial linguistic communication and social intelligence. TRENDS in Microbiology. 2004 Aug 1;12(8):366-72.
53. Morris MK, Saez-Rodriguez J, Sorger PK, Lauffenburger DA. Logic-based models for the analysis of cell signaling networks. Biochemistry. 2010 Apr 20;49(15):3216-24.
54. Gardner TS, Cantor CR, Collins JJ. Construction of a genetic toggle switch in Escherichia coli. Nature. 2000 Jan;403(6767):339-42.

 doi:10.20944/preprints202207.0110.v1

55. Siuti P, Yazbek J, Lu TK. Synthetic circuits integrating logic and memory in living cells. Nature biotechnology. 2013 May;31(5):448-52.
56. Padirac A, Fujii T, Rondelez Y. Bottom-up construction of in vitro switchable memories. Proceedings of the National Academy of Sciences. 2012 Nov 20;109(47):E3212-20.
57. Wang B, Kitney RI, Joly N, Buck M. Engineering modular and orthogonal genetic logic gates for robust digital-like synthetic biology. Nature communications. 2011 Oct 18;2(1):1-9.
58. Hill AV. The possible effects of the aggregation of the molecules of haemoglobin on its dissociation curves. j. physiol.. 1910;40:4-7.
59. O'Brien EL, Van Itallie E, Bennett MR. Modeling synthetic gene oscillators. Mathematical biosciences. 2012 Mar 1;236(1):1-5.
60. Fernando CT, Liekens AM, Bingle LE, Beck C, Lenser T, Stekel DJ, Rowe JE. Molecular circuits for associative learning in single-celled organisms. Journal of the Royal Society Interface. 2009 May 6;6(34):463-9.
61. Zorzan I, López AR, Malyshava A, Ellis T, Barberis M. Synthetic designs regulating cellular transitions: Fine-tuning of switches and oscillators. Current Opinion in Systems Biology. 2021 Mar 1;25:11-26.
62. Fitzgerald M, Gibbs C, Shimpi AA, Deans TL. Adoption of the Q transcriptional system for regulating gene expression in stem cells. ACS synthetic biology. 2017 Nov 17;6(11):2014-20.
63. Linsker R. Local synaptic learning rules suffice to maximize mutual information in a linear network. Neural Computation. 1992 Sep 1;4(5):691-702.
64. Higham NJ. Accuracy and stability of numerical algorithms. Society for industrial and applied mathematics; 2002 Jan 1.
65. Burden RL, Faires JD, Burden AM. Numerical analysis. Cengage learning; 2015.
66. Dormand JR, Prince PJ. A family of embedded Runge-Kutta formulae. Journal of computational and applied mathematics. 1980 Mar 1;6(1):19-26.
67. Ye H, Daoud-El Baba M, Peng RW, Fussenegger M. A synthetic optogenetic transcription device enhances blood-glucose homeostasis in mice. Science. 2011 Jun 24;332(6037):1565-8.
68. Kalos M, June CH. Adoptive T cell transfer for cancer immunotherapy in the era of synthetic biology. Immunity. 2013 Jul 25;39(1):49-60.
69. Krivonosov M, Nazarenko T, Bacalini MG, Zaikin A, Ivanchenko M, Franceschi C. Network markers of DNA methylation in neurodegenerative diseases. In2020 4th Scientific School on Dynamics of Complex Networks and their Application in Intellectual Robotics (DCNAIR) 2020 Sep 7 (pp. 138-139). IEEE.
70. Krivonosov M, Nazarenko T, Bacalini MG, Franceschi C, Zaikin A, Ivanchenko M. DNA methylation changes with age as a complex system: a parenclitic network approach to a family-based cohort of patients with Down Syndrome. bioRxiv. 2020 Jan 1.
71. Rössger K, Charpin-El Hamri G, Fussenegger M. Reward-based hypertension control by a synthetic brain–dopamine interface. Proceedings of the National Academy of Sciences. 2013 Nov 5;110(45):18150-5.